How to Cite: Vissurkhanova, Ya.A., Ivanova, N.M., Soboleva, Ye.A., & Muldakhmetov, Z.M. (2026). Comparison of the Influence of Polymer Additives on the Thermal and Electrochemical Reduction of Copper Ferrites and Electrocatalytic Activity of the Formed Fe-Cu Composites. *Eurasian Journal of Chemistry, 31, 3(123), 117–128.* https://doi.org/10.31489/2959-0663/3-26-6

Article

Received: 1 June 2026 | Revised: 14 August 2026 |
Accepted: 24 August 2026 | Published online: 28 August 2026

UDC 546.562+541.64+546.562+544.653.3 https://doi.org/10.31489/2959-0663/3-26-6

Yakha A. Vissurkhanova[1,2*], Nina M. Ivanova[1], Yelena A. Soboleva[1], Zainulla M. Muldakhmetov[1]

[1]*LLP "Institute of Organic Synthesis and Coal Chemistry of the Republic of Kazakhstan", Karaganda, Kazakhstan*
[2]*Buketov Karaganda National Research University, Karaganda, Kazakhstan*
*(*Corresponding author's e-mail: yakhavisurkhanova@bk.ru)*

Comparison of the Influence of Polymer Additives on the Thermal and Electrochemical Reduction of Copper Ferrites and Electrocatalytic Activity of the Formed Fe-Cu Composites

The conducted studies compared the influence of polymers (PVA, PVP, PEG and g-C_3N_4) added to the copper(II) and iron(III) cations co-precipitation environment during the preparation of copper(II) ferrite precursors on the phase compositions of $CuFe_2O_4$ + Polymer samples heat-treated at 700 °C, their electrochemical reduction, and the electrocatalytic activity of the resulting Fe-Cu composites. The structure and morphological features of $CuFe_2O_4$ + Polymer samples after heat treatment (HT) and electrochemical experiments were studied using XRD analysis and electron microscopy. Thermogravimetric studies were performed for the polymers and copper ferrite precursors. The results indicate that the thermal degradation products of PVA and g-C_3N_4 polymers induce a partial decomposition of copper ferrites during HT, yielding crystalline phases of copper and iron, thereby significantly decreasing the duration of the subsequent electrochemical reduction of these samples. "Pure" $CuFe_2O_4$ and samples containing other polymers remain stable at 700 °C. Electrochemical reduction of $CuFe_2O_4$ + PVP and $CuFe_2O_4$ + PEG samples result in a more complete reduction of iron cations than in other samples, which is favourable for intensifying the electrohydrogenation of 4-nitrophenol on Fe-Cu composites formed from these samples. The fabrication of a single product, 4-aminophenol, is confirmed by UV-vis spectra.

Keywords: copper ferrite, polymer additives, co-precipitation, heat treatment, electrochemical reduction, Fe-Cu composites, electrocatalytic hydrogenation, 4-nitrophenol

Introduction

Copper ferrite (II) ($CuFe_2O_4$) is a typical iron-based cubic spinel with high chemical stability, moderate non-toxicity, low cost, and excellent magnetic properties [1, 2]. Copper ferrite, like other transition metal ferrites, is widely utilized in applications ranging from environmental remediation and drug delivery to high-density magnetic storage and catalysis [3–6]. Copper ferrite nanoparticles are used as catalysts in classical thermocatalytic and electrocatalytic processes. The properties of copper ferrite are highly dependent on the synthesis parameters, such as the Fe/Cu ratio, calcination temperature and time, and the use of different stabilizers of copper ferrite nanoparticles or their supports.

Copper ferrite is produced by various methods, the main ones being ceramic technologies using metal oxide powders, CuO and Fe_2O_3 [7, 8]. However, these methods are quite laborious, especially when producing nanosized samples. In methods such as sol-gel, hydro/solvothermal, co-precipitation, and others, various organic compounds, including polymers, are often used to stabilize copper ferrite nanoparticles. For example, paper [9] describes the production of copper(II) ferrite nanoparticles by a hydrothermal method, in which salts of both metals were dissolved in an aqueous solution of ethylene glycol, then the pH of the mixture was adjusted to 12 using sodium hydroxide and it was kept at 180 °C for 6 h. It was found that with an increase in the ethylene glycol content in the reaction mixture, crystalline phases of $CuFe_2O_4$ and Cu are present in the composite. The appearance of copper is explained by the interaction of ethylene glycol with sodium hydroxide and the subsequent reduction of copper cations from copper(I) oxide.

Copper(II) ferrite was also prepared by the sol-gel method using a polymer (the so-called simple polymer-assisted sol-gel method) [10]. For this purpose, copper(II) and iron(III) nitrates in stoichiometric ratios were added to an aqueous solution of polyvinylpyrrolidone. The mixture was then kept at 80 °C until a gel-like precipitate formed, which was then kept at 250 °C for 15 min to remove organic components. The pre-

cipitate thus prepared was heat-treated at 750 and 950 °C. As a result, ferrite $CuFe_2O_4$ with a tetragonal structure was obtained, which also contained crystalline phases of CuO and Fe_2O_3 in small quantities. It was established that elevated temperatures and extended calcination durations promote the complete crystallization of copper ferrite, which simultaneously causes the nanoparticles to sinter into large agglomerates exceeding 1 μm in size. Furthermore, previous findings [11] regarding solid-phase synthesis with sodium oxalate and polyethylene glycol indicate that $CuFe_2O_4$ undergoes partial degradation into copper(II) and iron(III) oxides when temperatures surpass 400 °C. Soluble impurities were specifically removed before heat treatment at 400 °C.

Copper ferrite samples were produced by autocombustion using natural honey as a reducing and stabilizing agent [12]. Precursors synthesized by co-precipitation of copper and iron cations with sodium hydroxide in the presence of honey were treated at 400 and 800 °C for 4 h. The authors explained the voids between copper ferrite particles by the release of gaseous substances (N_2 and CO_2) formed as a result of the decomposition of glucose and fructose contained in honey. Moreover, the copper ferrite obtained at 400 °C contained crystalline phases of $CuFe_2O_4$ and oxides CuO and α-Fe_2O_3, whereas after heat treatment at 800 °C the sample was single-phase and contained only $CuFe_2O_4$ [12]. That is, no reduced metals were detected in the copper ferrite samples.

In [13], $CuFe_2O_4$ nanoparticles were synthesized by co-precipitation in an aqueous solution with the addition of polyethylene glycol. The resulting precipitate was thoroughly washed, dried, and then treated at 700ºC in a flow of oxygen in a tubular furnace. X-ray diffraction analysis revealed the presence of CuO, Fe_2O_3, and Fe_3O_4 oxides in the $CuFe_2O_4$ samples, the formation of which was explained by the oxidation of copper precipitated by polyethylene glycol, and insoluble FeO. A copper ferrite sample, the precursors of which were dried in a microwave oven, contained fewer impurities.

The given examples show that the addition of organic compounds to the reaction environment for the synthesis of copper ferrite promotes the stabilization of its nanoparticles and the appearance of both metals oxides, and, in rare cases, reduced metals in its composition. Apparently, this is due not only to the heat treatment temperature, the removal of impurities before heat treatment, or the heat treatment conditions, but also to the nature of the added organic stabilizers. In our previous studies devoted to the creation of Fe-Cu composites based on copper ferrite, it was found that the synthesis of copper ferrite by the method of co-precipitation of copper and iron cations in the presence of polymers [14] and carbon nanomaterials [15] followed by heat treatment leads to a change in its phase composition with the formation of not only oxides of both metals, but also reduced metals. Of course, this method is not a suitable synthesis option for obtaining stable crystalline copper ferrite, but for carrying out further electrochemical reduction of copper ferrite to produce catalytically active Fe-Cu composites, the introduction of such additives contributes to a noticeable decrease in the duration of the metal cations reduction process.

The present work aims to investigate the effect of polymer additives such as polyvinyl alcohol (PVA), polyvinylpyrrolidone (PVP), polyethyleneglycol (PEG) and graphitic carbon nitride (g-C_3N_4) on the structural changes in copper ferrite samples under thermal treatment at 700 °C. Additionally, the electrochemical reduction of both metals to form of Fe-Cu composites and their electrocatalytic activity in the model electrohydrogenation of 4-nitrophenol were analyzed.

Experimental

Materials

Copper(II) nitrate trihydrate ($Cu(NO_3)_2 \cdot 3H_2O$), iron(III) nitrate nonahydrate ($Fe(NO_3)_3 \cdot 9H_2O$) and sodium hydroxide (NaOH) were supplied by "Ridder" LLP (Karaganda, Kazakhstan). Dicyandiamide (CAS 461-58-5), polyvinyl alcohol (CAS 9002-89-5, 9,000-10,000 Mw), polyvinylpyrrolidone (CAS 9003-39-8, 10,000 Mw) and polyethylene glycol (CAS 25322-68-3, 10,000 Mw) were purchased from Sigma-Aldrich (USA) and used as received without further purification.

Synthesis of Graphitic Carbon Nitride g-C_3N_4

Graphitic carbon nitride g-C_3N_4 was synthesized following a previously reported procedure [15]. Briefly, 6 g of dicyandiamide was heated under an ambient air atmosphere to 550 °C and held at this temperature for 3 h. The obtained yellow product was ground into a fine powder.

Synthesis of Copper Ferrite and its Samples with Polymer Additives

Syntheses of "pure" copper ferrite and its samples with polymer additives (PVA, PVP, PEG, or g-C_3N_4) were performed by co-precipitation of metal cations from their nitrate salts and subsequent heat treatment (HT) using procedures similar to those described in our previously published works [14, 15]. The HT temperature (700 °C) and its duration (2 hours) for the prepared copper ferrite sample precursors were selected based on previously obtained results on the change in phase compositions of similar samples during HT.

Electrochemical and Electrocatalytic Experiments

Copper ferrite samples prepared with and without the addition of the polymers to the co-precipitation reaction medium and subsequent heat treatment were first reduced in an electrochemical cell. The resulting Fe-Cu composites were then used as electrocatalysts in the electrohydrogenation of 4-nitrophenol (4-NPh). The details regarding the electrochemical and electrocatalytic experiments can be found in our previous study [15]. The initial concentration of 4-NPh in the alcohol-aqueous-alkaline catholyte was 0.162 mol/L.

Characterization

Thermogravimetric measurements (TGA) were performed on a LabSYS evo TGA/LTA/DSC analyzer (Setaram Instrumentation, France). The samples were heated from 25 to 900 °C at a constant heating ramp of 10 °C/min under an air atmosphere. To identify the crystalline phases of the prepared composites, XRD analysis was carried out on a Rigaku SmartLab diffractometer (Rigaku, Japan) with CuKα radiation. The diffraction data were collected over a 2θ span of 5-90°. Their morphological features were studied on a TESCAN MIRA 3 (Tescan, Czech Republic) scanning electron microscope using secondary (SE) and backscattered (BSE) electron detectors. Elemental microanalysis of the samples was performed using an X-Act energy dispersive detector (Oxford Instruments, UK). Surface morphology of $CuFe_2O_4$ + g-C_3N_4 (700 °C) samples were studied using a scanning electron microscope JSM-IT 800 (JEOL, Japan). The samples were analyzed after deposition of conductive gold layer. The formation of 4-aminophenol as a product of electrocatalytic hydrogenation of 4-nitrophenol was established by its UV-Vis spectra recorded in the 250-500 nm wavelength range on a SHIMADZU UV-1900i spectrophotometer (Japan).

Results and Discussion

Figure 1 illustrates the chemical structures of the polymers employed to stabilize the copper ferrite precursor nanoparticles, which consist of copper and iron oxides and hydroxides formed during the co-precipitation of metal salts.

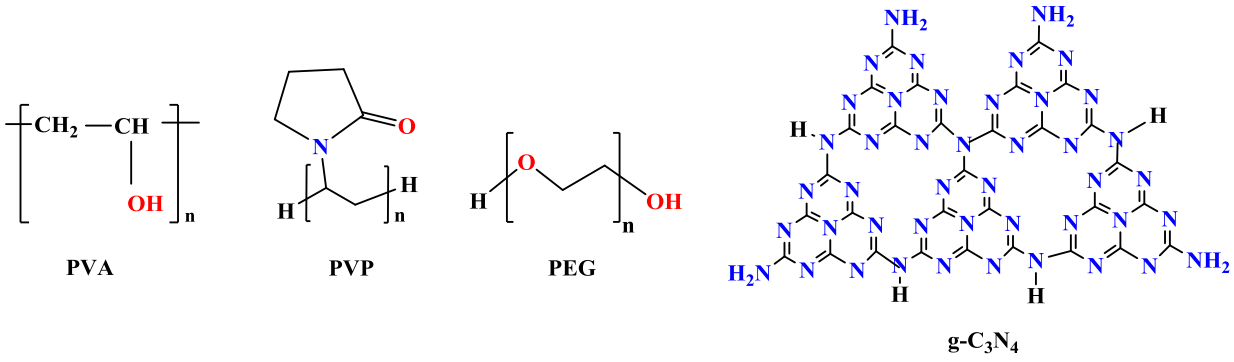

Figure 1. Structural formulas of the polymeric stabilizers employed during copper ferrite precursor synthesis

The PVA, PVP, and PEG polymers are characteristically known for their solubility in water. When the resulting precursors are washed, some of these polymers are removed, leaving behind, apparently, the portion that interacts with the precursor particles at the molecular level. The possibility of such an interaction was demonstrated by quantum-chemical calculations using the example of the PVA + $(CuO)_n$ system (n = 1-4) [16]. It was found that PVA is adsorbed on the surface of copper oxide particles through van der Waals and coordination interactions, as well as intramolecular hydrogen bonding. Polymeric graphitic carbon nitride, g-C_3N_4, on the contrary, is stable in an aqueous-alkaline environment, and the resulting precursors are deposited on its layered surface, reminiscent of graphite sheets [17, 18]. Therefore, graphitic carbon nitride not only acts as a stabilizer for copper ferrite precursor particles, but also serves as their carrier.

During heat treatment of the prepared precursors, the behaviour of the polymer stabilizers remaining after synthesis also varies. According to thermogravimetric analysis in air (Figure 2, curve *1*), the main decomposition of the PVA polymer occurs in the temperature range of 290-450 °C with a loss of ~80 % of the initial mass. The main products of the thermal-oxidative decomposition of PVA are water, acetaldehyde, carbon oxides (CO and CO_2), ethanol and other organic compounds, and at temperatures above 500 °C there are methane and hydrogen [19, 20].

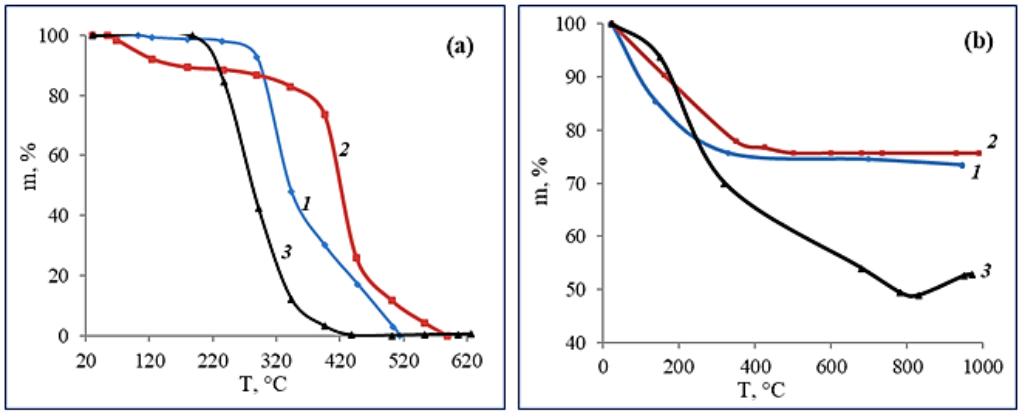

Figure 2. TG curves for (a) PVA (*1*), PVP (*2*), PEG (*3*) polymers; (b) $CuFe_2O_4$ (*1*), $CuFe_2O_4$ + PVP (*2*), $CuFe_2O_4$ + PVA (*3*) in the air

The TGA data (Figure 2(a), curve *2*) reveals that the primary degradation of the PVP polymer takes place between 320 and 450 °C, accompanied by a mass loss of ~75 %. The decomposition products are pyrrolidone, CO_2, hydrocarbons of various structures, and traces of ammonia [21, 22]. Above 450 °C, oxidation processes occur, releasing CO_2 and H_2O and completely burning the residue. Thermal decomposition of PEG polymer in air occurs at lower temperatures than that of PVA and PVP polymers: it begins at ~200 °C, indicating the low molecular weight of the polymer, and is almost fully completed to 390 °C (Figure 2, curve *3*). The main products of its decomposition in this temperature range can be aldehydes (formaldehyde, acetaldehyde), formic acid, ethylene glycol, methanol, ethanol, water, CO_2, CO, etc. [23].

According to the TGA experiment, graphitic carbon nitride produced by treating with dicyandiamide at 550 °C remains stable up to almost 512 °C (Figure 3, curve 1). It then decomposes almost completely to 835 °C, leaving behind approximately 5 % nitrogen-doped carbon (N-C).

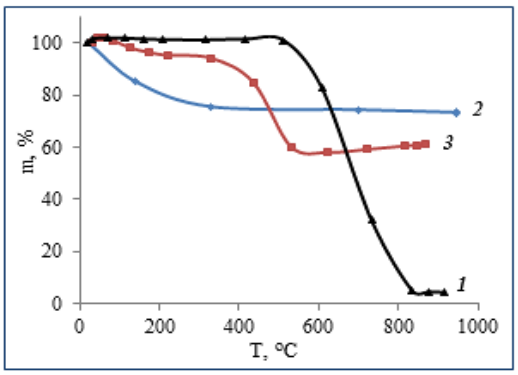

Figure 3. TG curves for g-C_3N_4 (*1*), $CuFe_2O_4$ (*2*), $CuFe_2O_4$ + g-C_3N_4 (*3*)

It can be assumed that all existing impurities (for example, NaOH) and the decomposition products of polymer stabilizers can influence the formation of the ferrite structure, weakening interatomic interactions and leading to the detachment of O_2 and reduction of metal cations.

The thermal behavior of the prepared copper ferrite precursors synthesized with and without the addition of polymer stabilizers, was also studied using TGA. Figure 2(b) shows that the $CuFe_2O_4$ and $CuFe_2O_4$ + PVP samples experience mass losses of 25 % and 22 % of the initial mass at temperatures up to 320-350 °C, respectively, whereas the $CuFe_2O_4$ + PVA samples experience a mass loss of 30 % of the initial mass. This is

due to the removal of their contained water and its loss during the transformation of metal hydroxides into their oxides. Metal ferrites then form as a result of the interaction of their oxides. With a further increase in temperature, the structures of the formed copper ferrites in the $CuFe_2O_4$ and $CuFe_2O_4$ + PVP samples remain unchanged and remain stable up to 950-990 °C. In contrast, in the $CuFe_2O_4$ + PVA sample, the mass loss continues up to 830 °C reaching almost 50 %, confirming the partial degradation of the copper ferrite itself. For the $CuFe_2O_4$ + g-C_3N_4 sample (Figure 3, curve *3*), a major weight loss step of ~40 % was recorded within the 330–530 °C thermal interval, which points to an incomplete decomposition of the ferrite.

The phase compositions of "pure" copper ferrite and its samples synthesized in the presence of polymers and then heat-treated at 700 °C were determined using X-ray diffraction analysis. At 700 °C, a solid-state reaction occurs between the copper and iron oxides, leading to the formation of the ferrimagnetic copper ferrite phase according to the following equation:

$$CuO + Fe_2O_3 \xrightarrow{700°C} CuFe_2O_4 \quad (1)$$

As copper ferrite is a stable ferrimagnetic phase under these conditions, its formation induces the magnetic response of the resulting composite. Therefore, the heat treatment at 700 °C does not cause a loss of magnetism, but rather enables the synthesis of the magnetically active phase from the initial amorphous metal oxides and hydroxides. As a result, the "pure" $CuFe_2O_4$ sample contains crystalline phases of cubic copper ferrite itself and a small amount of copper(II) oxide (Figure 4, (a)).

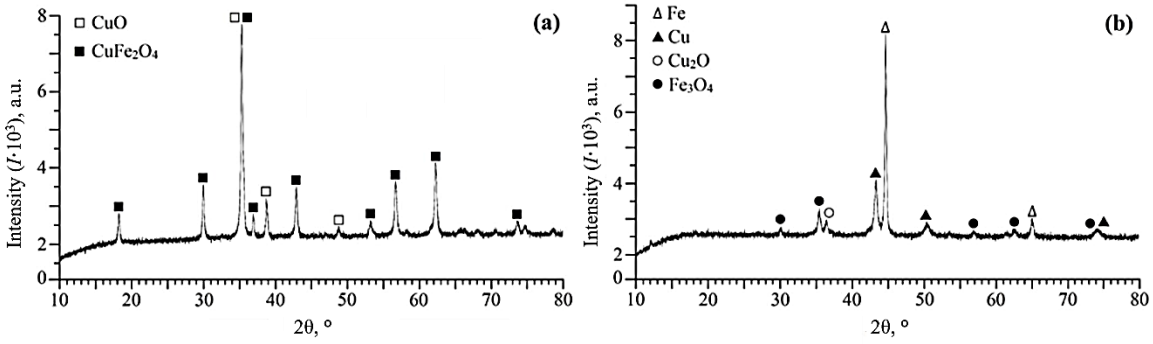

Figure 4. XRD patterns of $CuFe_2O_4$ (a) after HT at 700 °C and (b) after electrochemical experiments

The X-ray diffraction (XRD) pattern (Figure 5, 1(a)) indicate that heat-treating the $CuFe_2O_4$ + PVA precursor causes partial copper ferrite decomposition, generating reduced crystalline phases of Cu^0 and Fe^0 with well-defined, intense peaks. In addition to the remaining copper ferrite, this sample may also contain iron oxide Fe_3O_4 (magnetite), all of whose peaks overlap with those of $CuFe_2O_4$. The formation of Fe_3O_4 occurs as a result of the decomposition of copper ferrite, apparently under the influence of PVA decomposition products and other impurities (e.g., NaOH): $3CuFe_2O_4 \rightarrow 3Cu^0 + 2Fe_3O_4 + 2O_2$. According to [24], high-temperature reduction of Fe_3O_4 with a gas mixture (H_2/CO) occurs stepwise, through the formation of FeO (wüstite), which is then reduced to pure iron.

XRD patterns of $CuFe_2O_4$ + PVP (Figure 5, 2(a)) and $CuFe_2O_4$ + PEG (Figure 5, 3(a)) samples show that they contain crystalline phases of copper ferrite, copper(II) oxide, and small amounts of iron oxides, Fe_2O_3, and FeO. Apparently, PVP and PEG polymers are more soluble in water than PVA, and when the samples prepared after synthesis are washed, most of them are lost to the filtrates, and the concentration of the remaining polymers is insufficient to affect the copper ferrite and decompose it.

During the preparation of precursors for the $CuFe_2O_4$ + g-C_3N_4 sample, graphitic carbon nitride was taken in a 1:1 mass ratio to the theoretical yield of copper ferrite. After thermal treatment at 700 °C, according to XRD analysis, only ~15 % of the carbon remaining in the sample, formed from g-C_3N_4, with possible nitrogen doping (N-C). The XRD pattern of this sample, taken after thermal treatment, shows (Figure 5, 4(a)) that, as with the copper ferrite sample with PVA, the heat treatment process leads to partial copper ferrite decomposition, generating metallic copper and iron phases. The resulting composite also incorporates copper (I, II) oxides, carbon, and residual $CuFe_2O_4$ alongside co-existing Fe_3O_4.

In the electrochemical cell, under the specified conditions, copper ferrite is reduced to form crystalline phases of copper and iron, as confirmed by XRD analysis (Figure 5, 1(b)-4(b)). As follows from the XRD patterns, iron cations are more completely reduced in the $CuFe_2O_4$ + PVP and $CuFe_2O_4$ + g-C_3N_4 samples, which follows from the comparatively lower content of Fe_3O_4 oxide in these samples (Figure 5, 2(b) and

4(b)). Copper cation reduction is more complete in the $CuFe_2O_4$ + PVA and $CuFe_2O_4$ + g-C_3N_4 samples, according to the absence of Cu_2O oxide in their compositions after electrochemical experiments (Figure 5, 1(b) and 4(b)).

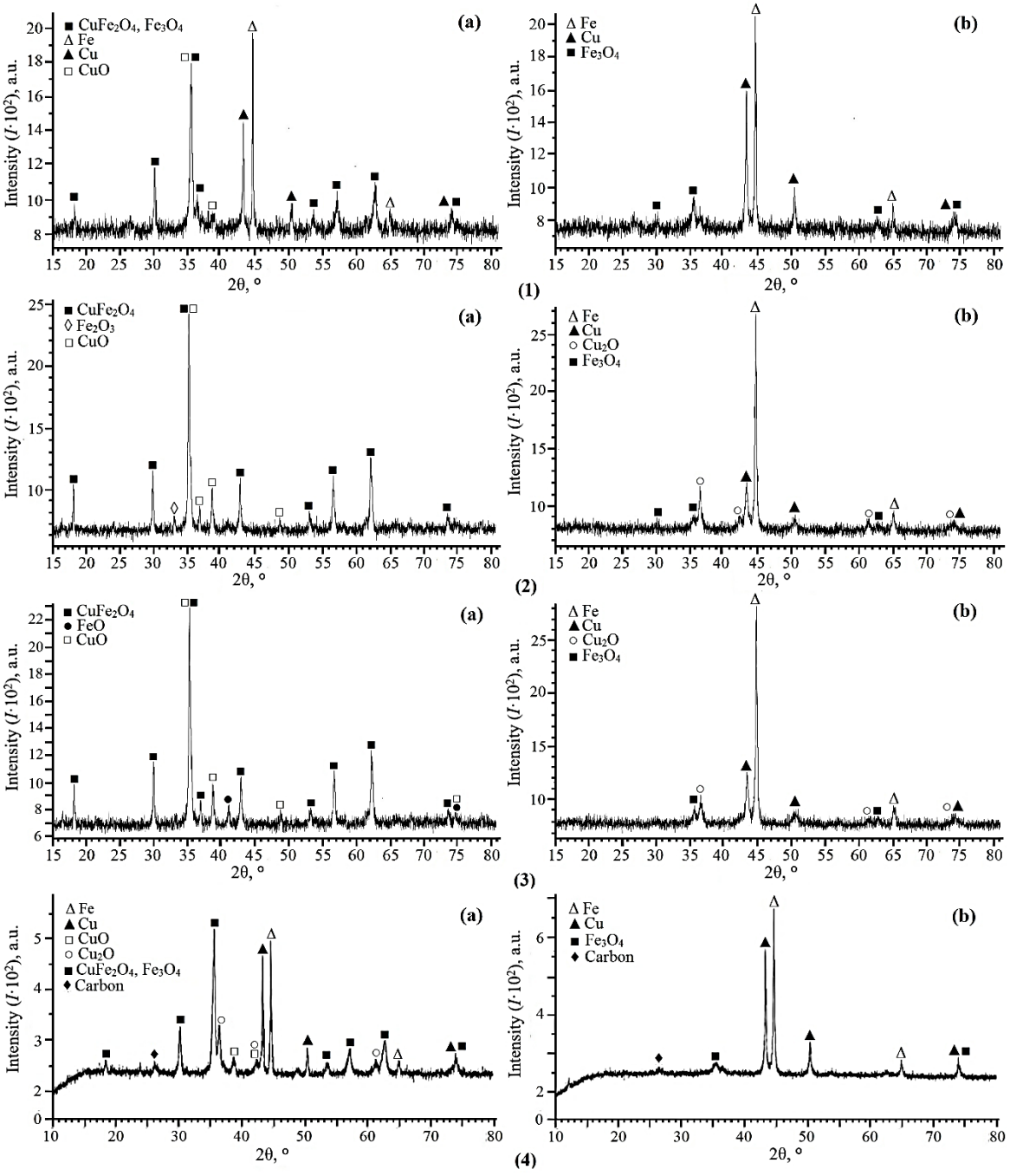

Figure 5. XRD patterns of $CuFe_2O_4$ + PVA (**1**), $CuFe_2O_4$ + PVP (**2**), $CuFe_2O_4$ + PEG (**3**), and $CuFe_2O_4$/g-C_3N_4 (**4**) after HT at 700 °C (a) and (b) after electrochemical experiments

Figures 6–9 display the SEM images of the copper ferrite samples prepared in the presence of polymer additives and annealed at 700 °C. The micrographs were taken using two electron detectors: a secondary electron (SE) detector, which allows one to study the relief and topography of the sample surface, and a backscattered electron (BSE) detector, which provides information on compositional contrast, i.e., areas with heavy elements appear brighter in the image than lighter elements. The BSE image of the C $CuFe_2O_4$ + PVA sample (Figure 6) contains areas of varying brightness: dark areas, apparently belonging to oxygen-containing compounds ($CuFe_2O_4$, Fe_3O_4), and lighter areas containing metallic particles, as established by

XRD analysis (Figure 5, 1(a)). EDS analysis also revealed areas of this sample's particles with higher and lower oxygen contents, and revealed a small carbon content (point spectra in Figure 6).

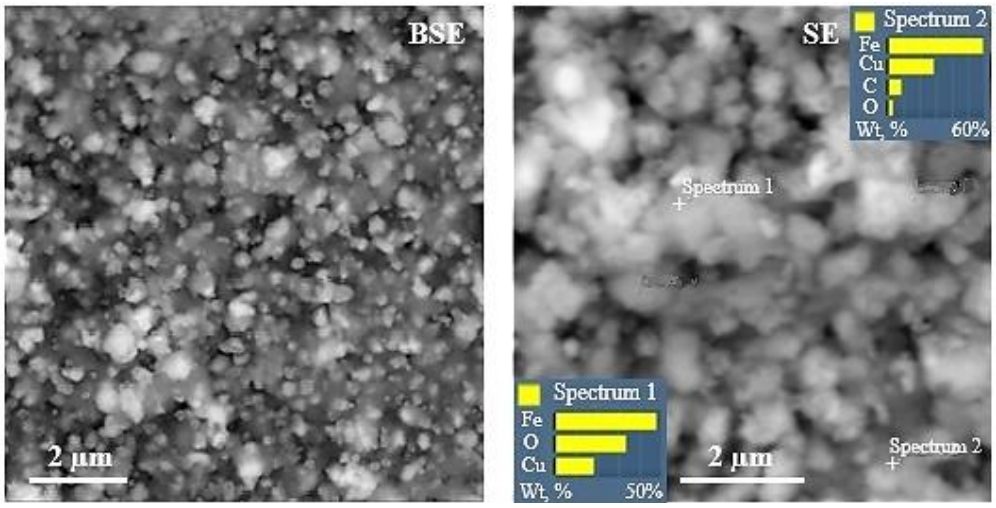

Figure 6. SEM images of $CuFe_2O_4$ + PVA (700 °C) sample

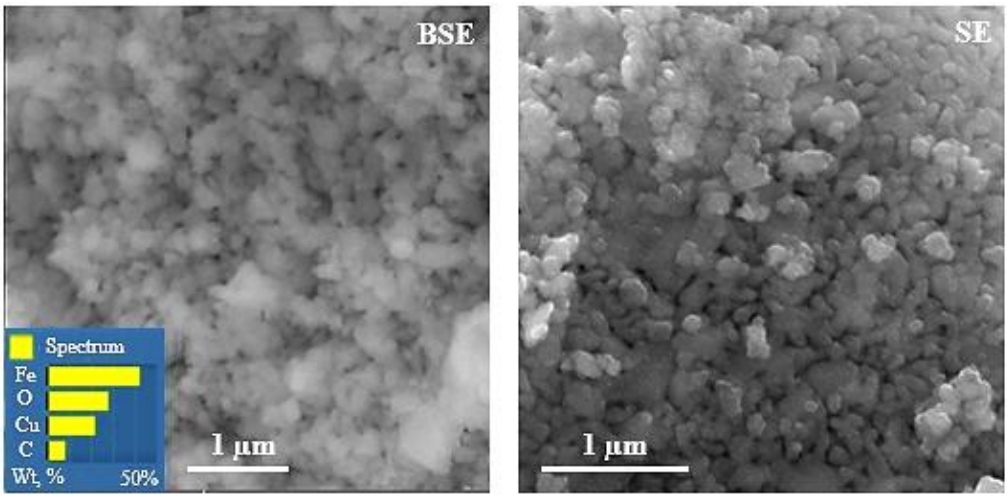

Figure 7. SEM images of $CuFe_2O_4$ + PVP (700 °C) sample

The $CuFe_2O_4$ + PVP and $CuFe_2O_4$ + PEG samples in BSE images (Figures 7 and 8) appear more compositionally uniform compared to the $CuFe_2O_4$ + PVA sample and consist primarily of copper ferrite particles. These particles are composed of smaller rounded or plate-like formations and resemble short sausages shaped to merge with each other, forming a hole in the centre (torus-like). In the $CuFe_2O_4$ + PEG sample (Figure 8), these toroidal formations are smaller. EDS analysis revealed the presence of carbon in both of these samples.

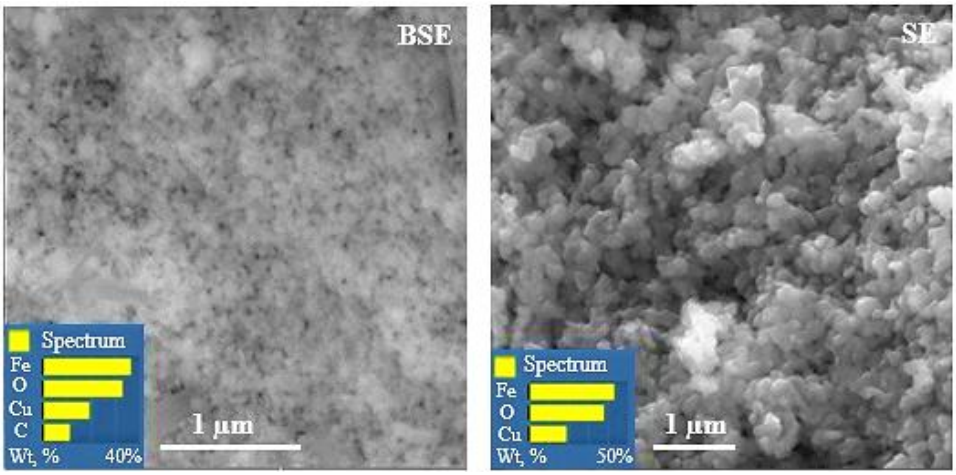

Figure 8. SEM images of $CuFe_2O_4$ + PEG (700 °C) sample

According to SE images of the $CuFe_2O_4$ + g-C_3N_4 sample (Figure 9), its composition contains particles of varying sizes and shapes: tetragonal pyramids of copper ferrite, layered formations of graphitic carbon nitride residues, and large balls twisted from plate-like copper oxide formations. EDS analysis of the selected area revealed a relatively high carbon content and a negligible nitrogen content (spectrum in the SE micrograph in Figure 9). This diverse composition of this sample after thermal treatment is well confirmed by its XRD analysis (Figure 5, 4(a)).

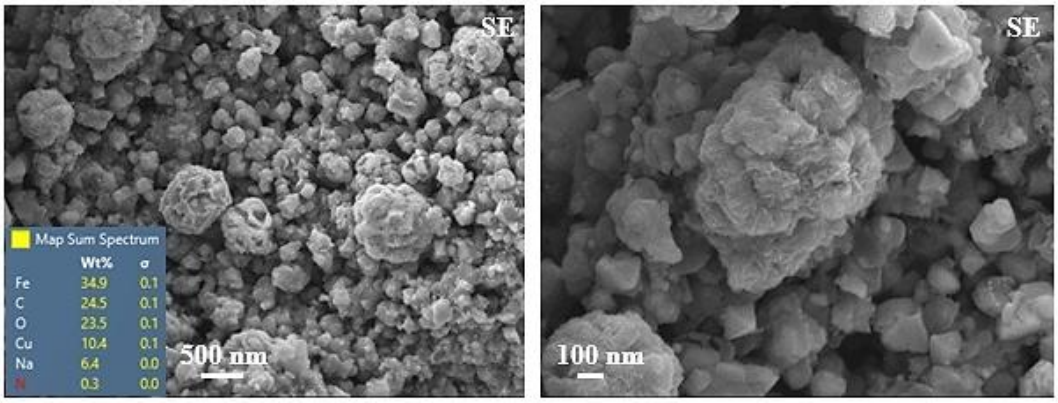

Figure 9. SEM images of $CuFe_2O_4$ + g-C_3N_4 (700 °C) sample

The copper ferrite samples prepared with and without the addition of polymers and obtained after thermal treatment were first reduced in an electrochemical cell. The Fe-Cu composites formed during the reduction were then tested for electrocatalytic activity in the electrohydrogenation of 4-nitrophenol. Notably, 4-NPh is classified as a pollutant, and its reduced form, 4-aminophenol, is a feedstock for the production of several pharmaceuticals, including paracetamol. Therefore, 4-NPh is a frequent subject of catalytic studies, primarily using sodium borohydride as a reducing agent [25-27].

Table 1 presents the results of the studies on the electrochemical reduction (EChR) of heat-treated copper ferrite samples and the electrocatalytic hydrogenation of 4-NPh on Fe-Cu composites. The key parameters evaluating both electrochemical processes are listed below: their durations (t_1 and t_2), the volume of oxygen released (ΔV_{O2}) in the copper ferrite EChR processes, the average 4-NPh hydrogenation rate (W) during the initial period (α = 0.25), the hydrogen utilization coefficient (η), close in its values to the faradaic efficiency, and 4-NPh conversion (α). Table 1 presents the experimental data expressed as the arithmetic mean values ($\bar{X}$) ± standard deviation (±δ) calculated across four independent runs (n = 4) calculated using well-known methods for the statistical processing of experimental data. For comparison, the parameters characterizing 4-nitrophenol electrochemical reduction on a bare copper cathode (in the absence of catalyst composites) are summarized in Table 1.

Table 1

Electrochemical reduction of copper(II) ferrite composites and electrocatalytic hydrogenation of 4-nitrophenol using Fe-Cu containing composites

Copper ferrite samples	EChR of copper ferrite samples		Electrocatalytic hydrogenation of 4-NPh			
	t_1, min	ΔV_{O2}, mL	t_2, min	W, mL H_2/min	η, %	α, %
Cu cathode	–	–	95.00±5.77	5.15±0.13	31.23±1.94	95.45±0.86
$CuFe_2O_4$, 700 °C	170.00±8.16	146.18±3.25	35.00±5.77	14.78±0.28	89.50±1.89	98.38±0.68
$CuFe_2O_4$ + PVA, 700 °C	70.00±8.16	96.25±2.43	35.00±5.77	14.90±0.29	89.54±1,78	98.40±0.63
$CuFe_2O_4$ + PVP, 700 °C	200.00±8.16	156.55±4.00	35.00±5.77	14.95±0.84	91.35±3.83	97.65±1.80
$CuFe_2O_4$ + PEG, 700 °C	208.75±8.54	153.70±6.62	35.00±5.77	15.70±0.55	93.75±3.20	97.10±2.06
$CuFe_2O_4$(1) + g-C_3N_4(1), 700 °C	95.00±9.13	115.78±8.72	36.30±4.79	13.20±0.79	80.15±5.17	97.68±1.72

The XRD data confirm that under the specified conditions, the thermally treated copper ferrite samples deposited on a Cu cathode undergo reduction, yielding Fe-Cu composites that still retain minor metal oxide residues (Figures 4(b) and 5, 1(b)-4(b)). As was shown previously [14], the electrochemical reduction of cations of both metals occurs in parallel. Possible electronic processes with the formation of assumed intermediate copper and iron oxides are described in a recently published article [15]. From the data in Table 1 it follows that the duration of electrochemical reduction of copper ferrite in the studied samples differs significantly. Shorter values of EChR duration are found for the copper ferrite samples synthesized using PVA and g-C_3N_4 polymers, i.e. these are just the ones that, during heating at 700 °C, underwent partial decomposition with the formation of copper and iron in a zero-valent state (Figure 5, 1(b) and 4(b)). In the samples with PVP and PEG polymers, in which thermal decomposition of copper ferrites did not occur (Figure 5, 2(b) and 3(b)), on the contrary, the EChR duration even increased slightly compared to pure $CuFe_2O_4$, which is also stable at 700 °C (Figure 4, (b)). This, firstly, may indicate a retarding effect of the carbon-containing residues of these polymers on the electrochemical reduction of metal cations in copper ferrite. Secondly, the recorded volumes of oxygen, released in addition to the volumes of H_2 and O_2 gases in a 2:1 ratio, also increased slightly, which may indicate more complete reduction of metal cations compared to the pure copper ferrite.

Electrochemical reduction of 4-NPh on a Cu cathode under the given conditions occurs at a rate of 5.15±0.21 mL/min, has a long duration, and has a fairly high degree of 4-NPh conversion (95.45±1.37 %) (Table 1). It can be assumed that this process is accompanied by the formation of by-products, which is typical for nitro compounds in an electrochemical system [28]. However, the UV-Vis spectra of the diluted catholyte after 4-NPh electrohydrogenation (Figure 10, (b), curve *2*) show the presence of a small amount of unreacted 4-NPh (a broad peak in the region of 403 nm) and a high content of 4-aminophenol (4-APh) (a peak in the region of 313 nm). For comparison, Figure 10, (a) shows the UV-vis spectra for aqueous-alkaline solutions of pure 4-NPh and 4-APh compounds. The use of Fe-Cu composites as electrocatalysts in this process, firstly, promotes a nearly threefold acceleration in the 4-NPh hydrogenation rate, thereby substantially shortening the reaction duration; secondly, the 4-NPh conversion reaches its maximum values. The absence of the initial 4-NPh in the catholytes after electrocatalytic hydrogenation on Fe-Cu composites formed from $CuFe_2O_4$ + PVA, $CuFe_2O_4$ + PEG, and pure $CuFe_2O_4$ samples is confirmed by UV-Vis spectra (Figure 10, (b)).

Among all copper ferrite samples, two samples, $CuFe_2O_4$ + PVA and $CuFe_2O_4$ + PEG, shown the highest 4-NPh hydrogenation rate (Table 1). The copper ferrites in these samples did not decompose during thermal treatment at 700 °C (Figures 5, 2(a) and 3(a)). As shown in the XRD patterns of these samples after electrochemical experiments (Figures 5, 2(b) and 3(b)), the diffraction peaks of the unreacted magnetite phase have the lowest intensity. Such a decline points to a near-total conversion of iron ions in these samples, and consequently, the highest content of reduced iron. This likely explains the highest rates of electrocatalytic hydrogenation of 4-NPh on Fe-Cu composites formed from these samples.

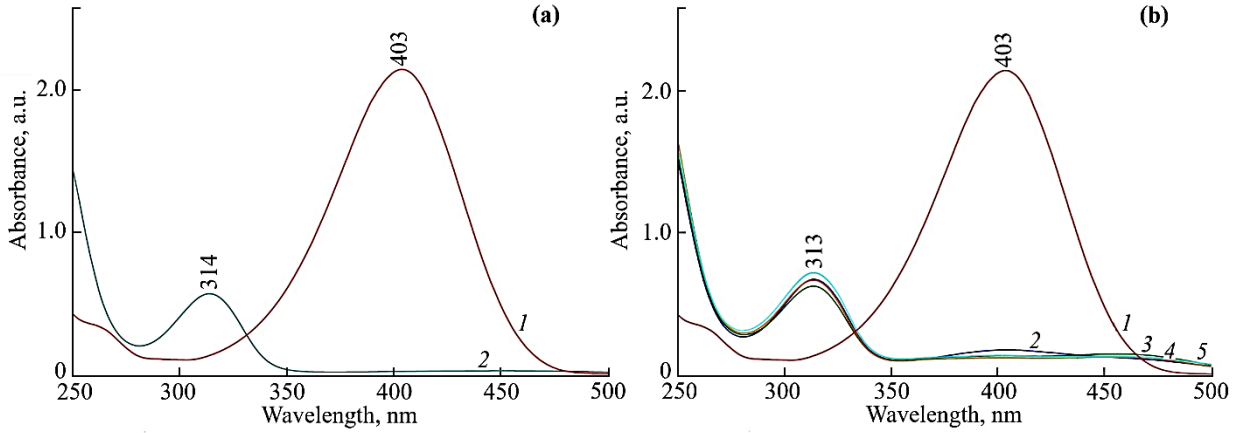

Figure 10. UV-vis spectra of (a) 4-NPh at the beginning of electrohydrogenation (*1*), and pure 4-APh (*2*); (b) catolyte with 4-NPh at the beginning of electrohydrogenation (*1*), catolyte after electrochemical reduction of 4-NPh (*2*), and catolytes after electrocatalytic hydrogenation of 4-NPh on the Fe-Cu composites based on (*3*) $CuFe_2O_4$ (700 °C), (*4*) $CuFe_2O_4$ + 3 % PVA (700 °C), and (*5*) $CuFe_2O_4$ + 3 % PVP (700 °C) samples

The samples synthesized using PVA and g-C_3N_4 polymers contained a large amount of reduced copper (based on the peak ratio in the 2θ = 43-45° angle range) already after the thermal treatment (Figure 5, 1(a) and 4(a)), which further increased after the electrochemical reduction of these samples. The resulting Fe-Cu composites demonstrated superior electrocatalytic performance during the electrohydrogenation of 4-nitrophenol, but slightly lower than that of the other composites (Table 1). Furthermore, it should be noted that the copper ferrite content in the $CuFe_2O_4$ + g-C_3N_4 (700 °C) sample was lower than that in the samples containing other polymers, and, therefore, the amount of reduced metals in the Fe-Cu composite formed from this sample was also lower. This apparently explains the some decrease in the rate of 4-NPh hydrogenation exhibited by this composite in the studied process compared to that of the other composites.

Conclusions

A comparison of the phase compositions of copper(II) ferrites synthesized by co-precipitation in the presence of a number of polymers (PVA, PVP, PEG, and g-C_3N_4) followed by heat treatment at 700 °C revealed the varying effects of these polymers on the subsequent transformation of the resulting copper ferrite samples. It was found that some polymers (PVA, g-C_3N_4) affect the phase compositions of the copper ferrites, leading to their partial decomposition during heat treatment, and their electrochemical reduction decreasing its duration. Other polymers (PVP, PEG) do not have this effect, but a more complete electrochemical reduction of iron cations in their copper ferrite samples prepared with their participation facilitates better intensification of 4-NPh electrohydrogenation with the formation of a single product, 4-aminophenol, which is of great practical importance. The different effects of the polymer additives discussed may be due to their structure, decomposition products during heat treatment, and their interaction with copper ferrite atoms. An additional factor influencing the copper ferrite transformations discussed may be the polymer concentration in co-precipitation reaction environment and their residual content in the copper ferrite precursors.

Funding

This research was funded by the Science Committee of the Ministry of Science and Higher Education of the Republic of Kazakhstan (Program No. BR24992921).

*Author Information**

**The authors' names are presented in the following order: First Name, Middle Name and Last Name*

Yakha Amkhadovna Vissurkhanova (*corresponding author*) — Researcher, Laboratory of Electrocatalysis and Quantum-chemical Research, LLP "Institute of Organic Synthesis and Coal Chemistry of the Republic of Kazakhstan", Alikhanov St., 1, 100000, Karaganda, Kazakhstan; Teacher, Department of Physical and Analytical Chemistry, Buketov Karaganda National Research University, Universitetskaya St., 28, 100024, Karaganda, Kazakhstan; e-mail: yakhavisurkhanova@bk.ru; https://orcid.org/0000-0001-7279-1145

Nina Mikhailovna Ivanova — Doctor of Chemical Sciences, Full Professor, Head of the Laboratory of Electrocatalysis and Quantum-chemical Research, LLP "Institute of Organic Synthesis and Coal Chemistry of the Republic of Kazakhstan", Alikhanov St., 1, 100000, Karaganda, Kazakhstan; e-mail: nmiva@mail.ru; https://orcid.org/0000-0001-8564-8006

Yelena Anatol'evna Soboleva — Candidate of Chemical Sciences, Associate Professor, Leading researcher, Laboratory of Electrocatalysis and Quantum-chemical Research, LLP "Institute of Organic Synthesis and Coal Chemistry of the Republic of Kazakhstan", Alikhanov St., 1, 100000, Karaganda, Kazakhstan; e-mail: esoboleva-kz@mail.ru; https://orcid.org/0000-0002-1089-367X

Zainulla Muldakhmetovich Muldakhmetov — Director of LLP "Institute of Organic Synthesis and Coal Chemistry of the Republic of Kazakhstan", Alikhanov St., 1, 100000, Karaganda, Kazakhstan; e-mail: iosu.rk@mail.ru; https://orcid.org/0000-0001-9497-2545

Author Contributions

The manuscript was written through contributions of all authors. All authors have given approval to the final version of the manuscript. CRediT: **Yakha Amkhadovna Vissurkhanova** investigation, methodology, data curation, visualization; **Nina Mikhailovna Ivanova** conceptualization, writing-original draft, methodology, validation, visualization, writing-review & editing; **Yelena Anatol'evna Soboleva** investigation, data curation, Figures design, resources, visualization; **Zainulla Muldakhmetovich Muldakhmetov** funding acquisition.

Conflicts of Interest

The authors declare no conflict of interest.

References

1 Rashad, M.M., Mohamed, R.M., Ibrahim, M.A., Ismail, L.F.M., Abdel-Aal, E.A. (2012). Magnetic and catalytic properties of cubic copper ferrite nanopowders synthesized from secondary resources. *Adv. Powder Technol., 23*, 315–323. https://doi.org/10.1016/j.apt.2011.04.005

2 Dey, A., Varshney, G., Maity, S., Sengupta, S. (2025). Hydrothermally synthesized ternary copper ferrite ($CuFe_2O_4$) micro-nano particles for high-capacity and long-life anodes in Li-ion batteries. *Mater. Lett., 401*, 139276. https://doi.org/10.1016/j.matlet.2025.139276

3 Wang, K., Yang, P., Guo, R., Yao, X., Yang, W. (2019). Photothermal performance of MFe_2O_4 nanoparticles. Chinese Chem. Lett., 30, 2013–2016**.** https://doi.org/10.1016/j.cclet.2019.04.005

4 Kharisov, B.I., Dias, H.V.R., Kharisova, O.V. (2019). Mini-review: Ferrite nanoparticles in the catalysis. *Arabian J. Chem., 12*, 1234–1246. http://dx.doi.org/10.1016/j.arabjc.2014.10.049

5 Dippong, T., Levei, E.A., Kadar, O. (2021). Recent advances in synthesis and applications of MFe_2O_4 (M = Co, Cu, Mn, Ni, Zn) nanoparticles. *Nanomaterials, 11*, 1560. https://doi.org/10.3390/nano11061560

6 Salih, S.J., Tahseen, Z.S. (2026). Spinel ferrite nanoparticles in environmental remediation: Adsorption, catalysis, and sustainability perspectives. *Next Sustainability*, *7*, 100240. https://doi.org/10.1016/j.nxsust.2025.100240

7 Goya, G.F., Rechenberg, H.R. (1998). Superparamagnetic transition and local disorder in $CuFe_2O_4$ nanoparticles. *Nanostruct. Mater*., *10*(6), 1001–1011. https://doi.org/10.1016/S0965-9773(98)00133-0

8 Marinca, T.F., Chicinaş, I., Isnard, O. (2012). Synthesis, structural and magnetic characterization of nanocrystalline $CuFe_2O_4$ as obtained by a combined method reactive milling, heat treatment and ball milling. *Ceram. Int.*, *38*(3), 1951–1957. https://doi.org/10.1016/j.ceramint.2011.10.026

9 Astaraki, H., Masoudpanah, S.M., Alamolhoda, S. (2021). Effects of ethylene glycol contents on phase formation, magnetic properties and photocatalytic activity of $CuFe_2O_4/Cu_2O/Cu$ nanocomposite powders synthesized by solvothermal method. *J. Mater. Res. Technol., 14*, 229–241. https://doi.org/10.1016/j.jmrt.2021.06.046

10 Calvo-de la Rosa, J., Segarra, M. (2019). Optimization of the synthesis of copper ferrite nanoparticles by a polymer-assisted sol-gel method. *ACS Omega*, *4*(19), 18289–18298. https://doi.org/10.1021/acsomega.9b02295

11 Wu, X., Zhou, K., Wu, W., Cui, X., Li, Y. (2013). Magnetic properties of nanocrystalline $CuFe_2O_4$ and kinetics of thermal decomposition of precursor. *J. Therm. Anal. Calorim*., *111*(1), 9–16. https://doi.org/10.1007/s10973-011-2104-6

12 Divakara, S. G., Jayanna, B. K., Mahesh, B., Anil Kumar, H. G., Reddy, M.A.H., Narasimhaswamy, N. (2026). Honey-assisted synthesis of $CuFe_2O_4$ nano pebbles: a sustainable approach to photocatalytic and antibacterial activity. *J. Exp. Nanosci*., *21*(1), 2630356. https://doi.org/10.1080/17458080.2026.2630356

13 Kanagaraj, M., Sathishkumar, P., Selvan, K., In, P., Arumugam, S. (2014). Structural and magnetic properties of $CuFe_2O_4$ as-prepared and thermally treated spinel nanoferrites. *Indian J. Pure Appl. Phys*., *52*(2), 124–130.

14 Ivanova, N.M., Soboleva, E.A., Visurkhanova, Ya.A., Muldakhmetov, Z. (2020). Electrochemical synthesis of Fe–Cu composites based on copper(II) ferrite and their electrocatalytic properties. *Russ. J. Electrochem.*, *56*, 533–543. http://doi.org/10.1134/S1023193520070034

15 Vissurkhanova, Ya.A., Ivanova, N.M., Soboleva, Ye.A., Muldakhmetov, Z.M. (2026). Fabrication and electrocatalytic activity of Fe-Cu/C composites based on copper ferrite modified with graphene oxide and graphitic carbon nitride. *Materials*, *19*, 2273. https://doi.org/10.3390/ma19112273

16 16. Vissurkhanova, Ya.A, Abulyaissova, L.K., Ivanova, N.M., Minaev, B.F. (2023). Molecular simulation of the interaction of polyvinyl alcohol with potential active centers of copper (II) oxide surface. *News of the Academy of Sciences of RK. Series Chemistry and Technology*, *457*(4), 54–68. https://doi.org/10.32014/2023.2518-1491.192

17 Zhu, J., Xiao, P., Li, H., Carabineiro S.A.C. (2014). Graphitic Carbon Nitride: Synthesis, Properties, and Applications in Catalysis. *ACS Appl. Mater. Interfaces*, *6*, 16449−16465. https://doi.org/10.1021/am502925j

18 Praus, P., Svoboda, L., Ritz, M., Troppova, I., Sihor, M., Koci, K. (2017). Graphitic carbon nitride: Synthesis, characterization and photocatalytic decomposition of nitrous oxide. *Mater. Chem. Phys.*, *193*, 438–446. https://doi.org/10.1016/j.matchemphys.2017.03.008

19 Taghizadeh, M.T., Yeganeh, N., Rezaei, M. (2015). The investigation of thermal decomposition pathway and products of poly(vinyl alcohol) by TG-FTIR. *J. Appl. Polym. Sci.*, *132*(25), 421177. https://doi.org/10.1002/APP.42117

20 Senkevich, S.I., Druzhinina, T.V., Kharchenko, I.M., Kryazhev, Yu.G. (2007). Thermal transformations of polyvinyl alcohol as a source for the preparation of carbon materials. *Solid Fuel Chem*., *41*, 45–51. https://doi.org/10.3103/S0361521907010107

21 Lorı´a-Bastarrachea, M.I., Herrera-Kao, W., Cauich-Rodrı´guez, J.V., Cervantes-Uc, J.M., Va´zquez-Torres, H., A´vila-Ortega, A. (2011). A TGA/FTIR study on the thermal degradation of poly(vinyl pyrrolidone). *A Therm. Anal. Calorim*., *104*, 737–742. https://doi.org/10.1007/s10973-010-1061-9

22 Jablonski, A.E., Lang, A. J., Vyazovkin, S. (2008). Isoconversional kinetics of degradation of polyvinylpyrrolidone used as a matrix for ammonium nitrate stabilization. Thermochimica Acta, 474(1-2), 78–80. https://doi.org/10.1016/j.tca.2008.06.003

23 Kou, Y., Wang, S., Luo, J., Sun, K., Zhang, J., Tan, Z., Shi, Q. (2019). Thermal analysis and heat capacity study of polyethylene glycol (PEG) phase change materials for thermal energy storage applications, *J. Chem. Thermodynamics*, *128*, 259–274. https://doi.org/10.1016/j.jct.2018.08.031

24 Cheng, H., Cao, G., Ba, Z., Hu, D., Wang, Y., Li, Ch., Zhao, J (2026). Magnetite reduction kinetics under H_2 and CO atmospheres at high temperature. *Korean J. Chem. Eng.*, *43*, 1493–1505. https://doi.org/10.1007/s11814-025-00643-6

25 Zhao, P., Feng, X., Huang, D., Yang, D., Astruc, D. (2015). Basic concepts and recent advances in nitrophenol reduction by gold- and other transition metal nanoparticles, *Coord. Chem. Rev.*, *287*, 114–136. https://doi.org/10.1016/j.ccr.2015.01.002

26 Din, M.I., Khalid, R., Hussain, Z., Hussain, T., Mujahid, A., Najeeb, J., Izhar, F. (2020). Nanocatalytic assemblies for catalytic reduction of nitrophenols: A critical review, *Crit. Rev. Anal. Chem.*, *50*(4), 322–338. https://doi.org/10.1080/10408347.2019.1637241

27 Mejía, Y.R., Bogireddy, N.K.R. (2022). Reduction of 4-nitrophenol using green-fabricated metal nanoparticles. *RSC Advances*, *12*(29), 18661–18675. https://doi.org/10.1039/d2ra02663e

28 Simonetti, S.O., Beil, S.B., Waldvogel S.R. (2025). Nitro substrates in reductive electrosynthesis: A review. *ACS Electrochem*., *1*, 805–818. https://doi.org/10.1021/acselectrochem.5c00081